Physica B: Condensed Matter 558 (2019) 65–73

Contents lists available at ScienceDirect

Physica B: Condensed Matter

journal homepage: www.elsevier.com/locate/physb

Review on the materials and devices for magnetic refrigeration in the temperature range of nitrogen and hydrogen liquefaction

Hu Zhang[a], Radel Gimaev[b,c], Boris Kovalev[b], Kamil Kamilov[d,e], Vladimir Zverev[d,*], Alexander Tishin[c,d]

[a] School of Materials Science and Engineering, University of Science and Technology of Beijing, Beijing 100083, PR China
[b] National Research Center "Kurchatov Institute", Moscow 123182, Russia
[c] Advanced Magnetic Technologies and Consulting LLC, Troitsk, Moscow 142191, Russia
[d] Faculty of Physics, M.V. Lomonosov Moscow State University, Moscow 119991, Russia
[e] Amirkhanov Institute of Physics DNC RAS, Makhachkala 367003, Russia

ARTICLE INFO

Keywords:
Magnetic refrigeration
Magnetocaloric effect
Gas liquefaction

ABSTRACT

Magnetic refrigeration based on magnetocaloric effect (MCE) has become a promising alternative technique to the traditional gas-compression refrigeration due to its friendly environment and high energy efficiency. In addition to room temperature magnetic refrigeration, this novel technology can be applied at low temperature, especially for the potential applications in gas liquefaction. Therefore, attention has been paid to explore suitable materials with large MCE near the gas liquefaction temperature and develop low temperature magnetic refrigerators. Herein, the typical magnetocaloric materials and prototypes in the temperature range of nitrogen and hydrogen liquefaction are reviewed. Heavy rare earth intermetallic compounds are promising for low temperature magnetic refrigeration due to a low ordering temperature and large magnetic moments. For example, DyFeSi compound shows a large reversible MCE under a low field change of 1 T around $T_C = 70$ K, which is near the liquefaction temperature of nitrogen (77 K). It has been proposed that a composite can be formed by a group of magnetic refrigeration materials with successive transition temperatures and nearly constant MCEs, therefore expanding the range of working temperature desirable for Ericsson-cycle magnetic refrigeration.

1. Introduction

Refrigeration and cryogenic technology play a very important role in improving modern living standards and work environment. Cooling technology has covered a wide range of aspects from domestic air conditioning and refrigerator to industrial gas liquefaction and scientific research. The electrical power consumption for cooling in its various forms accounts for more than 15% of total use of electric energy [1]. This consumption can reach 30% in developed countries [2,3]. Moreover, as more people around the world use air conditioning, its sale is estimated to grow by 20% per year [4]. At present, the predominant cooling technique is the conventional gas compression-expansion refrigeration, which had been commercialized for more than 100 years. However, even the best commercial conventional refrigerator units can only attain 40% of ideal Carnot efficiency [5,6]. Therefore, improving the energy efficiency of refrigeration technology is of vital importance for the control of energy consumption. On the other hand, the traditional cooling techniques use some harmful refrigerants. For example, chlorofluorocarbons (CFCs) and hydrochlorofluorocarbons (HCFCs) were used as refrigerant gases, but they were found to be highly damaging to the ozone layer that protects the earth from the intense rays of the sun. Therefore, the utilization of these refrigerants has been restricted according to the Montreal protocol since 1987 [7]. Alternatively, hydrofluorocarbons (HFCs) are increasingly used in place of ozone depleting refrigerants. However, the global warming potential (GWP) of HFCs is over 1000 times than that of CO_2; as greenhouse gases they are still not environmental friendly [8]. In 1997, Kyoto protocol has been adopted in order to reduce the greenhouse gas emissions [9]. In 2015, the United Nations Climate Change Conference announced that the global warming will be reduced to $< 2\,^{\circ}C$ by year 2100 [10]. In order to achieve this goal, the participating countries sought to limit the emission of greenhouse gases by using more zero-carbon technologies. Consequently, the search for new refrigeration technology with high energy efficiency and environmental friendly is urgent.

The magnetocaloric effect (MCE) is an intrinsic magneto-

* Corresponding author.
E-mail addresses: gimaev_rr@nrcki.ru (R. Gimaev), vi.zverev@physics.msu.ru (V. Zverev).

https://doi.org/10.1016/j.physb.2019.01.035
Received 20 August 2018; Received in revised form 16 December 2018; Accepted 18 January 2019
Available online 22 January 2019
0921-4526/

thermodynamic phenomenon of the magnetic material in which the temperature is changed by exposure of the material to a magnetic field [11–13]. Total entropy S of the magnetic material is contributed by three parts, i.e., the magnetic entropy ΔS_M, the electronic entropy ΔS_e, and the lattice entropy ΔS_l [14,15]. The spins will align parallel to the magnetic field when a magnetic material is magnetized adiabatically which, in turn, lowers the contributions of ΔS_M and ΔS_e. Because total entropy of the system stays constant under an adiabatic condition, the lattice contribution ΔS_l increases oppositely to keep total S constant. This leads to the temperature increase due to the enhancement of lattice vibrations. Vice versa, the removal of the field causes spin randomization that results in an elevation of magnetic entropy and a decrease of lattice entropy; then the temperature of magnetic material decreases [16]. Based on MCE, magnetic refrigeration has been developed as a promising novel cooling technology, including high efficiency air conditioning in large buildings. In comparison with the traditional gas-compression refrigeration, magnetic refrigeration is advantageous in several aspects [14,17,18]: (i) the magnetic refrigeration materials and water-based heat transfer medium have no serious environmental problems; (ii) greater efficiency of a magnetic refrigerator comparing to conventional ones [6,19] (in case of maximum cooling power values); for example, in Ref. [20], for a magnetic refrigerator working at RT the value of cooling power (768 W) and 60% of ideal Carnot cycle efficiency are reached when a temperature span is about 20 K (see Table 2 in Ref. [20]); (iii) the magnetic refrigerator can be more compact and less noisy due to the use of solid materials and evading the compressor. Therefore, magnetic refrigeration has attracted worldwide interest.

However, it is worth noting that the cooling power of a magnetic refrigerator depends on the temperature span. For devices that use single material AMR, temperature span increase leads to an approximately linear decrease in the cooling power. In other words, the maximum cooling power values are reached at zero temperature span, and vice versa, at maximum temperature span, the cooling power goes to zero (see, for example, Fig. 1 in Ref. [21]). In most works the maximum valued of cooling power or cooling efficiency are presented, which are achieved at zero temperature span. Nevertheless, the work on increasing the cooling power and cooling efficiency at a significant temperature span is underway. One of the possible options to avoid the influence of the inverse linear dependence of the cooling power on the temperature span is to use of a regenerator consisting of several magnetic materials. This may lead to a change in the behavior of the temperature span - cooling power dependence (see Fig. 1 in Ref. [21]) and to the appearance of a region with a weak dependence of cooling power on the temperature span.

Dozens of research groups and industrial companies are working to improve magnetic cooling technology (to increase the efficiency of existing prototypes, develop silent devices, etc.) and develop new devices (in Ref. [22] 41 prototypes are described). Despite the fact that today the technology of magnetic cooling is experiencing certain difficulties when entering a very saturated market of refrigerators (which is typical for any new technology), there has been a significant progress in recent years. For example, in 2017, Cooltech Applications began commercial production of magnetic refrigerators and continues to work on increasing the cooling efficiency of a commercial model [20].

Historically, MCE has been discovered by Weiss and Piccard in 1917 who found that the change of magnetic field caused a temperature change in nickel around its Curie temperature (T_C) [23,24]. Later, Debye [25] and Giauque [26] independently proposed that MCE can attain very low temperature by adiabatically demagnetizing paramagnetic salts. In 1933, the first MCE application was experimentally demonstrated by Giauque and MacDougall to achieve a temperature of 0.25 K by adiabatic demagnetization of $Gd_2(SO_4)_3{\cdot}8H_2O$ [27]. Although the magnetic refrigeration gained much progress at low temperatures, the near-room temperature magnetic refrigeration had not been reported until 1976, when Brown demonstrated that a large temperature gradient of 46 K can be obtained under the magnetic field change of 7 T in pure Gd around 294 K [28]. Since then, efforts have been put to the room temperature magnetic refrigeration. In 1990, Nikitin et al. [29] reported MCE of $Fe_{49}Rh_{51}$ alloy which is the largest MCE ever achieved (12.9 K in $\Delta\mu_0 H$ = 1.95 K) [30]. The closest to this result values, obtained from direct measurements, are presented in Ref. [31] (9.2 K in 1.9 T). In Ref. [31] the estimations of ΔT (10,5–12 K in 1,9 T), obtained from ΔS_M data i.e. from indirect measurements are also presented. It should be noted that the magnetic properties and MCE in FeRh alloys strongly depend on structural defects, preparation procedures, heat treatment, measurements conditions [32–35], therefore, the available experimental data presented in literature can vary greatly.

Two major breakthroughs occurred in 1997. The Ames laboratory and Astronautics Corporation of America developed a proof-of-principle room temperature magnetic refrigeration device with maximum cooling power of 600 W at temperature span 10 K, magnetic field 5 T and flow rate 5 L/min [18]. It is worth noting that with a further increase of temperature span, the cooling power decreases linearly, thus at a temperature span of 22 K the cooling power is only 150 W. Furthermore, Pecharsky and Gschneidner reported the gigantic MCE in $Gd_5(Si, Ge)_4$ compounds around room temperature which exhibit a significantly higher MCE and tunable working temperature compared with Gd [36,37]. The discovery of large MCE in $Gd_5(Si, Ge)_4$ alloys dramatically accelerated the field of magnetic refrigeration worldwide.

Up to date, several other families of magnetic materials have been reported to show large MCEs near room temperature, such as $La_{1-x}Ca_xMnO_3$ manganites [38,39], La(Fe, Si)$_{13}$-based alloys [40,41], $MnAs_{1-x}Sb_x$ [42], MnFe(P, As) [43], Ni-Mn-based Heusler [44,45], and MM′X (M, M′ = transition metals, X = carbon or boron group elements) compounds [46,47]. Although these materials show much larger MCEs than Gd, they still cannot replace Gd due to “Non-MCE” properties, e.g., difficult preparation and fabrication, poor corrosion resistance, thermal and magnetic hysteresis, low thermal conductivity, high electrical resistance, and constant cycling stability [12]. Therefore, a great deal of effort has been made to improvement of performance for these materials in many aspects [48–52]. In addition to the room temperature cooling application, magnetic refrigeration also has a wide demands for low temperature cooling, especially the gas liquefaction. As one of the important low temperature refrigerants, liquid nitrogen is extensively used in low temperature physics, superconducting, medicine, etc. Hydrogen is considered as one of the most environmentally friendly energy sources for replacing the traditional non-renewable and polluting fossil fuels. Considering the high energy density and economy, liquid hydrogen is desired for transportation and storage of hydrogen. Magnetic refrigeration behaves with much higher thermal efficiency and entropy density of the refrigerants than the conventional liquefaction technique using the Joule-Thomson valve [11]. Though the adiabatic demagnetization of paramagnetic salts has become standard technique to attain very low temperatures, the magnetic refrigeration is still unavailable for liquefaction of nitrogen and hydrogen due to the lack of suitable magnetocaloric materials [53]. In recent years, some materials have been found to present large MCEs around the liquefaction temperature of nitrogen and hydrogen.

Importantly, excellent working bodies for this temperature range are rare earth orthoaluminates with a perovskite structure, such as $DyAlO_3$ and $Dy_xEr_{1-x}AlO_3$, that have advanced properties than garnets such as $Gd_2Ga_3O_{12}$, $Dy_2Ga_3O_{12}$, $Dy_2Ga_3O_{12}$ [54–58].

Herein we review recent progress on the magnetic refrigeration in the temperature range of nitrogen and hydrogen liquefaction (20–77 K). The review does not consider the helium temperature range which will be analyzed elsewhere.

2. Development of magnetic refrigeration materials in the temperature range of nitrogen and hydrogen liquefaction (20–77 K)

According to the thermodynamic theory, maximum magnetic

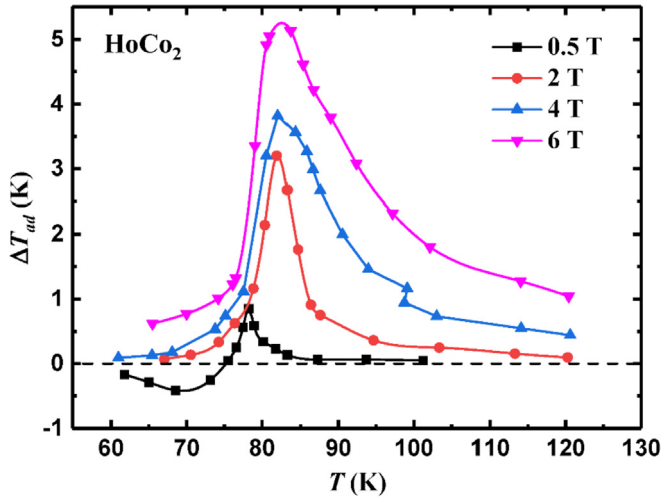

Fig. 1. Temperature dependence of the adiabatic temperature change (ΔT) for $HoCo_2$ compound under different magnetic field changes [63].

entropy change (S_M) per mole of magnetic ions is $S_M = R\ln(2J + 1)$, where R is the universal gas constant and J is total angular momentum of magnetic ion [14]. Thus, heavy rare earth intermetallic compounds are expected to exhibit a large MCE because of the high magnetic moments of heavy rare earth atoms. Moreover, most heavy rare earth intermetallic compounds have relatively low magnetic ordering temperature, suggesting their application in low temperature magnetic refrigeration [14,59]. The RCo_2 intermetallic compounds (R = rare earth) with cubic Laves-phase structure show first-order magnetic transition (FOMT) from paramagnetic (PM) to magnetically ordered state accompanied by a sharp increase of unit volume for R = Dy, Ho, Er, and so that implies the potential of high MCEs [60–62]. Nikitin et al. reported a large MCE in $HoCo_2$ [63]. Fig. 1 shows the temperature dependence of the adiabatic temperature change (ΔT) for $HoCo_2$ under different magnetic fields [63]. $HoCo_2$ undergoes a PM to ferromagnetic (FM)-like phase transition at T_C = 78 K, which is close to the nitrogen liquefaction temperature of 77 K, suggesting the potential applications for liquefaction of nitrogen. Maximum ΔT value of 5.1 K can be obtained around T_C under the field change of 6 T. The T_C peaks broaden asymmetrically toward high temperatures with the increase of magnetic field, indicating the occurrence of field-induced metamagnetic transition from PM to FM states. This metamagnetic transition is associated with the metamagnetism of Co sublattice, which is caused by the molecular field created by the localized 4*f* moments of Ho atoms [64,65]. In addition, a negative MCE (so-called inverse MCE) appears below T_C. This fact suggests the presence of AFM components below T_C, which leads to the higher magnetic entropy with the applied magnetic field. In other words, the inverse MCE signifies that the material can be cooled by adiabatic magnetization rather than adiabatic demagnetization. The inverse MCE manifests itself in the materials in the FOMT temperature range (AFM-FM, AFM - ferrimagnetic, collinear - noncollinear AFM transitions) [45], in which the inhomogeneities appear. In accordance with the exchange-inversion magnetism in FOMT [66] the change of magnetic ordering nature at the transition point is due to the fact that different types of exchange interactions simultaneously coexist in the material, differing in the size, sign, and dependence on interatomic distances. Such a mixture of coexisting exchange interactions leads to the fact that an increase in the external magnetic field disorders [45] spins, i.e., the magnetic part of the entropy increases, and the temperature decreases under adiabatic conditions.

Although the materials with FOMT, such as $HoCo_2$, show large MCEs due to the first-order metamagnetic transition, this is also accompanied by a remarkable thermal and magnetic hysteresis. On the contrary, the materials with second-order magnetic transition (SOMT) present reversible MCEs over a relatively broad temperature range in response to the variation of magnetic field desirable for practical applications. Therefore, a great number of SOMT materials have been searched to exhibit large MCE at low temperatures [58,67–69]. Dan'kov el al. reported that $DyAl_2$ undergoes SOMT from PM to FM states at T_C = 65 K [58]. $DyAl_2$ shows a ΔT_{ad} as high as 9.2 K for a field change of 7.5 T, which is much larger than ΔT_{ad} of 5.2 K for $GdAl_2$. The lower MCE of $GdAl_2$ is mainly due to two factors: (1) the magnetic entropy of Gd ion is 17.29 J/mol K, ~33% smaller than that of Dy ion (23.05 J/mol K); (2) the lattice heat capacity of $GdAl_2$ at its T_C = 167 K is higher than that of $DyAl_2$ at the T_C. $ErAl_2$ exhibits an even larger ΔT_{ad} of 14.5 K for a field change of 7.5 K around the T_C = 14 K. Based on that, one may expect that a series of $(Dy_{1-x}Er_x)Al_2$ compounds present large MCEs over a wide temperature range below 77 K by substituting Dy with Er, e.g., $(Dy_{0.4}Er_{0.6})Al_2$ shows a ΔT_{ad} of 10.4 K around the T_C = 31 K [58]. Of particular interest are Gd-based intermetallic compounds. Compositions with temperature-shifted points of magnetic phase transitions, e.g., $GdAl_2$ and Gd_3Al_2, can also be used in magnetic refrigerating machines [54,55,58].

The magnetic refrigerator can be more compact and cheaper if the magnetic field source is supplied by permanent magnets instead of superconducting magnets. However, at present the maximum field of permanent magnets is usually < 2 T. Therefore, it is necessary to search for the materials with large MCEs under low magnetic fields, especially lower than 2 T. In recent years, several series of ternary intermetallic *RTX* compounds (R = rare earth, T = transitional metal, X = *p*-block metal) have been found to exhibit large MCEs under relatively low magnetic field [68–71]. Among them, DyFeSi experiences a FM-PM SOMT at the T_C = 70 K, which is near the liquefaction temperature of nitrogen (77 K) [69]. Based on the Curie-Weiss fitting of magnetic susceptibility, the effective magnetic moment (μ_{eff}) of DyFeSi is obtained to be 11.41 μ_B. This μ_{eff} value is close to the free ion moments of Dy^{3+} (10.63 μ_B), indicating the absence of localized Fe magnetic moment. This fact is consistent with the results of other *RTX* [70,72]. Fig. 2(a) displays the magnetic entropy change ΔS_M as a function of temperature for DyFeSi compound under different magnetic fields [69]. Usually, the ΔS_M value can be calculated from the magnetization isotherms by using Maxwell relation $\Delta S_M(T, H) = \mu_0 \int_0^H (\partial M/\partial T)_H dH$ [73,74]. The validity of Maxwell relation has been debated intensively in the vicinity of FOMT due to the spurious ΔS_M spike, which is related to the history-dependent magnetic state [75–80]. In contrast, it is generally applicable for the SOMT. In addition, the ΔS_M can be also estimated from the heat capacity by using the equation $\Delta S_M(T) = \int_0^T [C_H(T) - C_0(T)]/TdT$ [73]. For comparison, the ΔS_M value under a field change of 2 T was calculated by both methods (heat capacity data is shown in the inset of Fig. 2(b)); ΔS_M values match well with each other. For relatively low field changes of 1 T and 2 T, the maximum $-\Delta S_M$ value of DyFeSi is 4.8 J/kg K and 9.2 J/kg K, respectively. This large ΔS_M value under low magnetic field change is practically favorable.

Zverev et al. [81] predicted that the maximum ΔT_{ad} value of MCE is 18 K/T for the ideal hypothetical binary compound based on general thermodynamic considerations. Any deviation from the ideal assumptions, such as non-optimal ΔS_M peak aspect ratio, dilution with non-magnetic atoms, or substituting rare earths with 3*d* elements, will inevitably lower the maximum ΔT_{ad}. Therefore, a magnetic refrigerant with ΔT_{ad} higher than the one of Gd (2.6–2.9 K/T) will be hardly found. In order to comprehensively evaluate MCE of DyFeSi, the ΔT_{ad} value was calculated using the equation $\Delta T_{ad} = -\Delta S(T, H) \times T/C_P(T, H_0)$, where $C_P(T, H_0)$ is zero-field heat capacity (inset of Fig. 2(b)). Fig. 2(b) displays the temperature dependence of ΔT_{ad} for DyFeSi compound under different magnetic field changes [69]. The maximum ΔT_{ad} value is 1.7 K and 3.4 K for the low field changes of 1 T and 2 T, respectively. MCE of DyFeSi is larger than those of other materials with similar working temperature, such as TbCoAl [82], Ho_5Si_4 [83], and EuO [84],

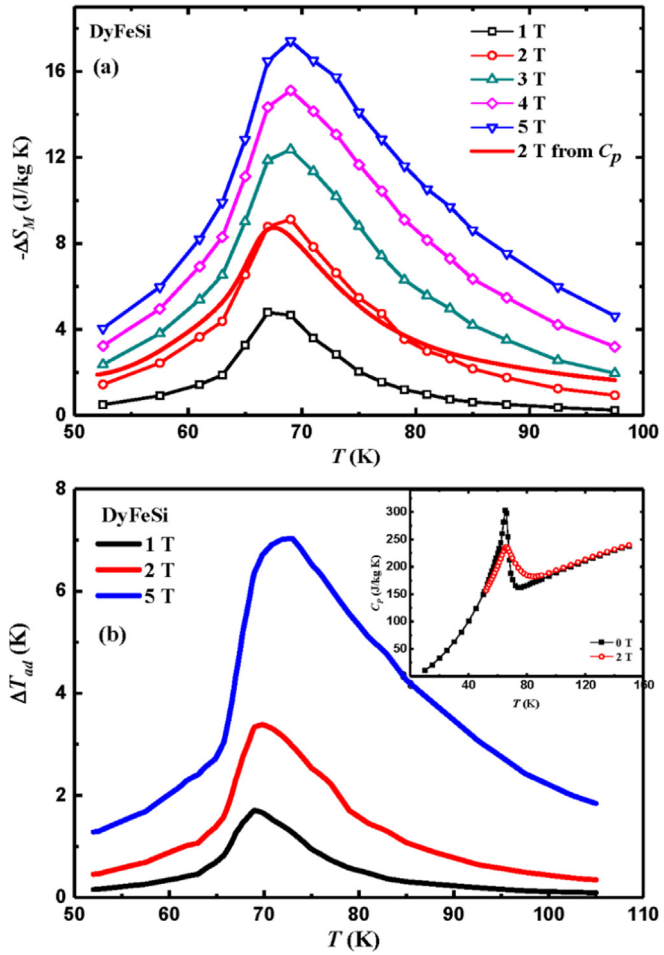

Fig. 2. Temperature dependence of (a) ΔS_M and (b) ΔT_{ad} for DyFeSi compound under different magnetic field changes. The inset shows the temperature dependence of heat capacities C_P for DyFeSi compound under 0 and 2 T [69].

suggesting the applicability of DyFeSi compound for magnetic refrigeration of nitrogen liquefaction.

In addition to DyFeSi compound, ErFeSi was found to undergo a second-order PM-FM transition at T_C = 22 K, which is near the liquid hydrogen temperature of 20 K [68]. Fig. 3 shows the temperature dependences of zero-field-cooling (ZFC) and field-cooling (FC) magnetizations for ErFeSi compound under 0.05 T [58]. The ZFC and FC curves are perfectly reversible around T_C as usually observed in the SOMT. However, the ZFC and FC curves show a large discrepancy below T_C. This thermomagnetic irreversibility is probably attributed to the domain wall pinning effect observed in the systems with high magnetocrystalline anisotropy and low ordering temperature [68,72,85]. In ZFC mode, the thermal energy is not strong enough to overcome the energy barrier since the domain walls are pinned, thus resulting in low magnetization. In contrast, the pinning effect is overcome by the magnetic field during the field-cooling process, so the magnetization below T_C becomes higher than that in ZFC mode. Fig. 4 shows the temperature dependence of (a) ΔS_M and (b) ΔT_{ad} of ErFeSi under different field changes [68]. Here, the ΔS_M value was calculated using Maxwell relation $\Delta S_M(T, H) = \mu_0 \int_0^H (\partial M/\partial T)_H dH$ [73,74], while the ΔT_{ad} was estimated from heat capacity curves by the equation $\Delta T_{ad}(\Delta H, T) = [T(S)_H - T(S)_0]_S$ [73]. For relatively low field change of 2 T, the maximum values of $-\Delta S_M$ and ΔT_{ad} are 14.2 J/kg K and 2.9 K, respectively. This large MCE indicate that ErFeSi can be an attractive magnetic refrigeration material for hydrogen liquefaction. Unlike the large MCE induced by coupled magnetic and structural transitions in FOMT materials, such huge MCE in ErFeSi with SOMT is mainly attributed to the sharp change of magnetization during magnetic transition [68]. It is worth noting that, as shown in Refs. [86,87], the refrigeration capacity and relative cooling power are simply not a good figure of merit of magnetocaloric materials.

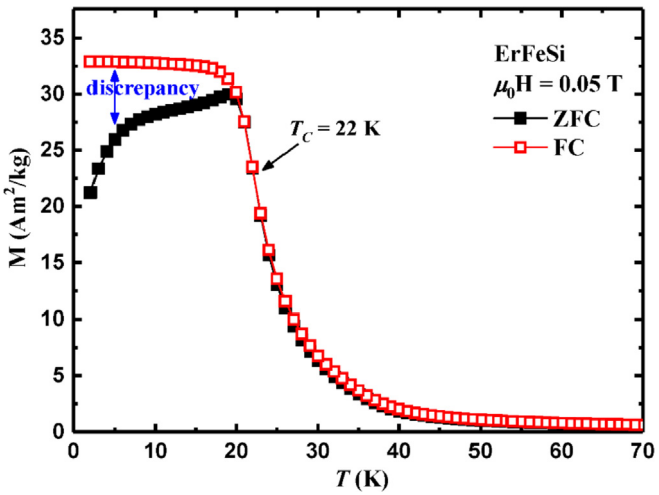

Fig. 3. Temperature dependences of zero-field-cooling (ZFC) and field-cooling (FC) magnetizations for ErFeSi compound under 0.05 T [68].

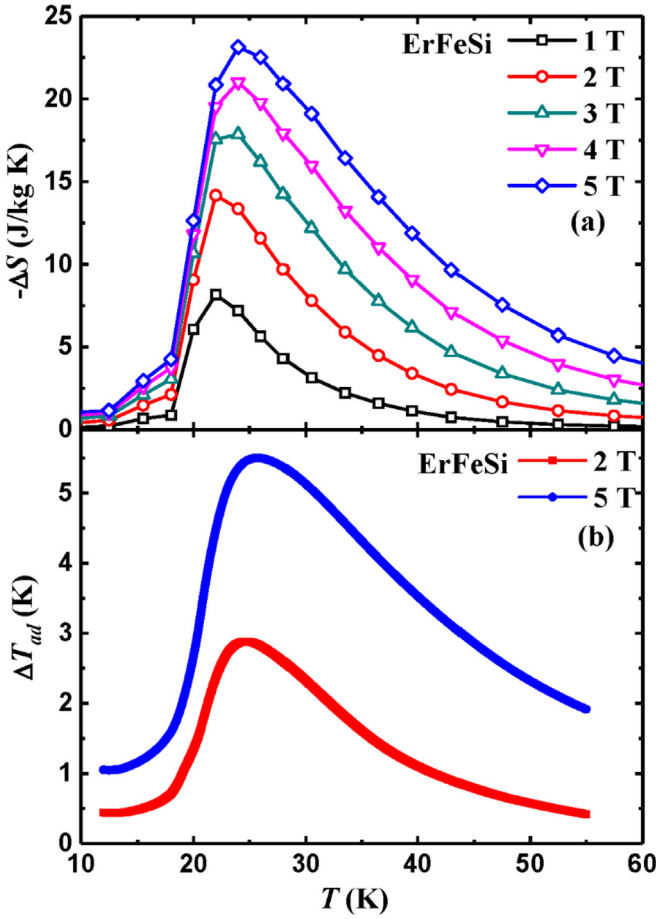

Fig. 4. The temperature dependence of (a) ΔS_M and (b) ΔT_{ad} for ErFeSi compound under different field changes [68].

Since only one material shows a significant MCE in the vicinity of the transition temperature, it is necessary to use a series of magnetocaloric materials with successive transition temperatures to expand the working temperature range of the magnetic refrigerator. Based on this

Table 1
Compositions of optimal refrigerants of rare earth alloys for three-stage Ericsson-type cycles overlapping the temperature range of 20–300 K. $T_{1\ int}$ and $T_{2\ int}$ are the temperatures of local cycle boundaries [88].

	Composition of the first refrigerant	$T_{1\ int}$, K	Composition of the second refrigerant	$T_{2\ int}$, K	Composition of the third refrigerant
1	$Gd_{0.6}Tb_{0.4}$	215	$Tb_{0.5}Dy_{0.5}$	135	Ho
2	$Gd_{0.7}Tb_{0.3}$	220	$Tb_{0.5}Dy_{0.5}$	115	Ho
3	$Gd_{0.4}Tb_{0.6}$	190	Dy	110	Ho
4	$Gd_{0.7}Tb_{0.3}$	250	$Tb_{0.6}Dy_{0.4}$	135	Ho

concept, Tishin proposed the composition of optimum working substances for magnetic refrigerator operating in 77–300 K temperature range [88]. The compositions of optimal refrigerants of rare earth alloys over the temperature range of 20–300 K have been suggested (Table 1). As seen from Table 1, Tb-Gd alloys were calculated to be the greatest effective in the high-temperature range; Dy and Tb-Dy alloys showed the most effect in the central cycle; and Ho element was a universal refrigerant in the low-temperature range.

In addition to the expansion of working temperature range, a constant ΔS_M as a function of temperature is another requirement for the ideal Ericsson-type cycle based on the thermodynamic analysis [14]. However, this goal is hard to be achieved by single magnetic material since the ΔS_M reduces quickly away from the transition temperature. On the contrary, it is suggested that the composite of several magnetocaloric materials with similar ΔS_M values could be the best choice to fulfil this requirement [89]. Zhang et al. found that TbFeSi and DyFeSi showed nearly the same magnitude of ΔS_M, i.e., the maximum ΔS_M values for a field change of 1 T are 5.3 J/kg K at $T_C = 110$ K and 4.8 J/kg K at $T_C = 70$ K for TbFeSi and DyFeSi, respectively [69]. Both TbFeSi and DyFeSi showed the same crystal structure with similar lattice parameters, so it is reasonable to choose a group of $(Tb_{1-x}Dy_x)FeSi$ compounds with successive ordering temperatures but similar ΔS_M values [90,91]. Assuming that (1) the T_C is proportional to the de Gennes factor [91], and (2) Tb^{3+} and Dy^{3+} ions do not have interactions [90], the T_C and ΔS_M values of $(Tb_{1-x}Dy_x)FeSi$ compounds can be calculated using the equations:

$$T_C = (1-x)T_{C_{Tb}} + xT_{C_{Dy}} \quad (1)$$

$$\Delta S(T,H) = (1-x)\Delta S_{Tb}\left(T_{C_{Tb}} + \Delta T, H\right) + x\Delta S_{Dy}\left(T_{C_{Dy}} + \Delta T, H\right) \quad (2)$$

where $T_{C_{Tb}}$ and $T_{C_{Dy}}$ are the T_Cs, and ΔS_{Tb} and ΔS_{Dy} are the ΔS_M values for TbFeSi and DyFeSi, respectively, and $\Delta T = T - T_C$. Fig. 5 presents the temperature dependence of calculated ΔS_M for $(Tb_{1-x}Dy_x)FeSi$ compounds under a magnetic field change of 1 T [69]. These compounds show the nearly constant magnitude of ΔS_M. Furthermore, a composite material can be formed based on this series of $(Tb_{1-x}Dy_x)FeSi$, and the optimum mass ratio y_i of each component obtained by a numerical method [69] was as follows: $y_1 = 19.43$ wt.%, $y_2 = 13.32$ wt.%, $y_3 = 13.47$ wt.%, $y_4 = 13.74$ wt.%, $y_5 = 15.08$ wt.%, and $y_6 = 24.96$ wt.% for $x = 0$, 0.2, 0.4, 0.6, 0.8, and 1.0, respectively. The ΔS_M of this composite was calculated to be 1.4 J/kg K under a field change of 1 T by using the equation $\Delta S_{com} = \sum_{i=1}^{6} y_i \Delta S_i$ and is shown in Fig. 5. This composite shows a constant ΔS_M over a broad temperature range of 67–108 K. However, as shown by theoretical calculations (see Fig. 5), the use of this approach reduces the maximum value of ΔS_M by more than three times. To eliminate this effect, in the design and manufacture of AMR beds, multilayer filling of AMR beds is carried out with materials with different Curie temperatures. At the same time, the layers of materials are filled in such a way that their Curie temperatures consistently increase from the cold end of the AMR bed to the warm end, so that each layer is in the temperature range closest to its Curie temperature. Schematic images of such a filling are shown, for example, in Fig. 3 of [92] and Fig. 6 of [93].

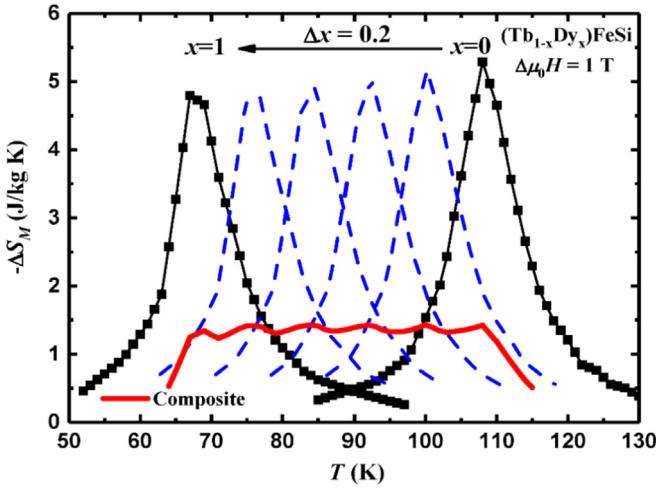

Fig. 5. Temperature dependence of calculated ΔS_M for $(Tb_{1-x}Dy_x)FeSi$ compounds and the composite material of $(Tb_{1-x}Dy_x)FeSi$ compounds under a field change of 1 T [69].

In addition to the materials discussed above, interest in magnetocaloric properties of rare earth based metal–organic framework materials has recently increased [94–96]. These materials may exhibit large values of magnetocaloric parameters at temperatures below liquid helium and, thus, promising for use in refrigerators operating at temperatures up to several kelvin. Magnetic molecular clusters may also be promising for use in refrigerators at helium temperatures [97].

3. Development of magnetic refrigerators in the temperature range of nitrogen and hydrogen liquefaction (20–77 K)

The majority of the existing magnetic cooling devices presented in literature are based on the regenerative cycle [5,18,22,74,98–100]. Non-regenerative cycles (the Carnot cycle) are used for devices operating at ultralow temperatures (below the temperature of liquid helium) [101–104], in which the Carnot cycle is the most effective.

Fig. 6 shows the dependences of entropy (S) on temperature (T) (S-T diagrams) for the Carnot, Brayton and Ericsson cycles typical for ferromagnetic materials. The upper curve S (T) in Fig. 6 corresponds to a material that is in a zero magnetic field (H = 0), and the lower one corresponds to a material that is in a magnetic field with a non-zero strength ($H \neq 0$). The rectangle ABCD represents the non-regenerative Carnot cycle. As one can see, the cycle includes two isentropic (AB and

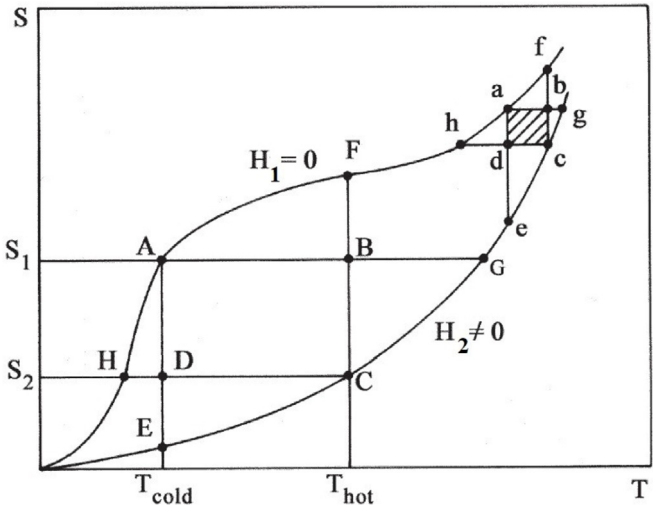

Fig. 6. S – T diagrams of the Carnot, Brayton and Ericsson cycles [14].

CD) and two isothermal (BC and DA) processes, while isentropic processes are realized when the magnetic field is changed (AF and EC correspond to a constant magnetic field).

Fig. 6 also presents the Ericsson regenerative (AFCE) and Brayton cycles (AGCH). Regenerative cycles include processes at a constant field, which makes it possible to take full advantage of the change in the magnetic part of the entropy generated when the magnetic field changes. In Ericsson cycle the magnetic field changes isothermally (FC and EA processes), and in Brayton cycle adiabatically (AG and CH processes), while the processes at constant field require thermal regeneration. The regenerator in a heat machine is a device for transferring heat between different parts of the cycle, which allows for an increase of the working temperature difference. This component of a heat engine stores heat in itself in the part of the cycle where heat is generated by the working material (body) and gives it up in the part where the working material absorbs it. This is especially important in the magnetic heat engine since the values of the adiabatic temperature change of magnetic materials are much smaller than the required working temperature difference. Therefore, the magnetic heat engine must have in its composition a regenerator in one form or another. The ferromagnetic material is heated by magnetization and cooled by demagnetization, which is a manifestation of the magnetocaloric effect. Therefore, in Fig. 6 thermal energy should be absorbed by the regenerator during processes in a non-zero magnetic field (CE and GC for Ericsson and Brayton cycles, respectively) and be given by the regenerator during processes in a zero magnetic field (AF and NA for Ericsson and Brayton cycles, respectively).

Another regenerative thermodynamic cycle used in magnetic heat engines is the active magnetic regenerative (AMR) thermodynamic cycle. In this cycle, the regenerator itself is a magnetic material, and the heat exchange in the regeneration process occurs between the magnetic material and the coolant, which eliminates the technical difficulties and losses associated with the use of a separate regenerator, as is assumed in devices with Ericsson and Brayton regenerative cycles.

At higher temperatures, including the considered range of 20–77 K, the Carnot cycle is not effective [14], since the entropy of solids at temperatures above 20 K will increase strongly. This leads to a decrease in the operating temperature span, which is limited to the ΔT of the working fluid and is several K for the Carnot cycle. Thus, regenerative cycles such as Brayton, Ericsson and AMR (active magnetic regenerator), which allow to increase the temperature span, have become the most widespread in devices operating at temperatures above 20 K. The Carnot cycle, as well as the Brayton, Ericsson and AMR cycles were discussed in detail in the reviews [14,93].

In Ref. [92] it is shown that, to realize the ideal Ericsson cycle, it is promising to use a complex working body consisting of several types of magnetic materials with different Curie temperatures in the range 20 K–60 K. A complex material consisting of RAl_2 layers, where R is Er, Ho and ($Ho_{0.5}Dy_{0.5}$) is described in Ref. [92].

Another way to increase the temperature span is associated with the use of two-stage AMR. In this case, in each AMR stage different magnetic materials are used as a working body and each AMR stage has its own operating range. Their combination in one cycle allows for extending the temperature span. Two-stage AMR was used by the authors of [105] in the active magnetic regenerative hydrogen liquefier, which can operate as a magnetic refrigerator between 77 and 20 K. The temperature region of the first stage operation was 39–77 K, and for the second stage – 19–39 K $GdNi_2$ (upper stage) and GdPd (lower stage) were used as working bodies. It should be noted that the authors used two moving superconducting magnets (fields values were 7 T and 5 T, respectively).

A similar scheme with two-stage AMR is also realized by the authors of [106,107] to create a prototype of a magnetic refrigerator operating in the temperature range 20–77 K (the temperature span is 57 K). Among the principal differences from the scheme proposed in Ref. [105] are: in each AMR stage, filling of bed with several materials is used (the first stage is filled by $GdNi_2$ and $Dy_{0.85}$ $Er_{0.15}$ Al_2 and the second stage is filled by $Dy_{0.5}$ $Er_{0.5}$ Al_2 and $Gd_{0.1}$ $Dy_{0.9}$ Ni_2). The magnetic field was created by AC superconducting magnet rather than moving the superconducting magnet. Common is also the use of the gaseous helium as a heat transfer fluid and the use of a liquid nitrogen as a cold heat-sink reservoir.

The results of numerical analysis of AMRs for hydrogen magnetic refrigeration between 20 K and 77 K are shown in Ref. [108]. The calculations were performed for the Brayton-like cycle case. The analysis was carried out for the cases: single layer AMR bed, two layered AMR bed, multi-stage AMR. The authors note that numerical analysis of the cycle plays an important role in understanding the processes in AMR.

Devices for hydrogen liquefaction have been reported that do not work on the AMR cycle but on the non-regenerative ADR cycle (adiabatic demagnetization refrigerator) close to the Carnot or the hybrid cycle, which includes the regenerative AMR and the non-regenerative cycles. In Ref. [109] shown is a magnetic refrigerator for hydrogen liquefaction working on a hybrid cycle consisting of the Carnot and AMR cycles. The AMR cycle is used to cool hydrogen gas to a temperature slightly higher than the boiling point. Furthermore, for transfer of hydrogen gas to the liquid phase, the Carnot cycle is used (the temperature span for the Carnot cycle is several K, so it is necessary to pre-cool the boiling points by the AMR cycle). A similar device in which the ADR cycle is used is presented in Ref. [110].

4. Conclusions and perspectives

Typical magnetic refrigeration materials and prototypes in the temperature range of nitrogen and hydrogen liquefaction (20–77 K) have been reviewed. According to the thermodynamic theory, heavy rare earth intermetallic compounds are generally expected to be the candidates for low temperature magnetic refrigeration due to the low ordering temperature and high magnetic moments of heavy rare earth atoms. Although large MCE can be contributed by the variation of both magnetic and lattice entropy in FOMT materials, the accompanied hysteresis loss is unfavorable. In contrast, SOMT materials show reversible MCE without hysteresis loss, and the large MCE is mainly attributed to the abrupt change of magnetization during magnetic transition. In order to enlarge the working temperature range, it has been proposed to use several numbers of local Ericsson-type cycles. Furthermore, a composite formed by a series of magnetocaloric materials with successive transition temperatures and similar magnitude of MCE is suggested to be desirable for Ericsson-cycle magnetic refrigeration.

Though a number of magnetocaloric materials with large MCE and prototypes with high performance have been reported in the temperature range of nitrogen and hydrogen liquefaction, there are still some issues that need to be overcome to realize the practical applications: (1) so far, a magnetic refrigerant with ΔT_{ad} higher than that of Gd (2.6–2.9 K/T) has still not been found yet; (2) the intermetallic compounds are usually quite brittle, so the fabrication technique and mechanical properties would be a serious obstacle that hinder the materials from applications; (3) In addition to MCE, thermal conductivity is an important factor which affects the ability of the magnetic refrigerant to transfer thermal energy to heat transfer liquid; (4) the corrosion behavior of magnetocaloric materials in the heat transfer liquid also needs to be evaluated. The above aspects are to be analyzed in future studies.

Acknowledgements

This work was supported by National Natural Science Foundation of China (Grant No.: 51671022); National Key Research and Development Program of China (Grant No.: 2017YFB0702704); Beijing Natural Science Foundation (No. 2162022); and Scientific and Technological Innovation Team Program of Foshan (2015IT100044). Work in

Advanced Magnetic Technologies and Consulting, LLC was supported by Skolkovo Foundation, Russia. The authors thank A. A. Shtil for editing the manuscript.

References

[1] A. Zhukov (Ed.), Novel Functional Magnetic Materials: Fundamentals and Applications, Springer International Publishing, 2016, http://www.springer.com/us/book/9783319261041 , Accessed date: 21 June 2018.

[2] S.F. Pearson (Ed.), 17th Informatory Note on Refrigerating Technologies: How to Improve Energy Efficiency in Refrigerating Equipment, International Institute of Refrigeration, 2003.

[3] M. Balli, S. Jandl, P. Fournier, A. Kedous-Lebouc, Advanced materials for magnetic cooling: fundamentals and practical aspects, Appl. Phys. Rev. 4 (2017) 021305, https://doi.org/10.1063/1.4983612.

[4] M.A. McNeil, V.E. Letschert, Future air conditioning energy consumption in developing countries and what can be done about it: the potential of efficiency in the residential sector, European Council for an Energy Efficient Economy Summer Study Proceedings, 2007, p. 1311.

[5] A. Kitanovski, J. Tušek, U. Tomc, U. Plaznik, M. Ozbolt, A. Poredoš, Magnetocaloric Energy Conversion: from Theory to Applications, Springer International Publishing, 2015, https://www.springer.com/la/book/9783319087405 , Accessed date: 21 June 2018.

[6] V. Franco, J.S. Bl´azquez, B. Ingale, A. Conde, The magnetocaloric effect and magnetic refrigeration near room temperature: materials and models, Annu. Rev. Mater. Res. 42 (2012) 305–342, https://doi.org/10.1146/annurev-matsci-062910-100356.

[7] See https://treaties.un.org/doc/Publication/UNTS/Volume%201522/volume-1522-I-26369-English.pdf for Montreal Protocol On Substances that Deplete the Ozone Layer, Concluded at Montreal on 16 September 1987, United Nations-Treaty Series.

[8] O. Sari, M. Balli, From conventional to magnetic refrigerator technology, Int. J. Refrig. 37 (2014) 8–15, https://doi.org/10.1016/j.ijrefrig.2013.09.027.

[9] See, for Kyoto Protocol to the United Nations Framework Convention on Climate Change, United Nations, 1998, http://unfccc.int/resource/docs/convkp/kpeng.pdf.

[10] Y. Gao, X. Gao, X. Zhang, The 2 °C global temperature target and the evolution of the long-term goal of addressing climate change—from the united Nations framework convention on climate change to the Paris agreement, Engineering 3 (2017) 272–278, https://doi.org/10.1016/J.ENG.2017.01.022.

[11] S.B. Roy, K.H.J. Buschow (Ed.), Handbook of Magnetic Materials, North-Holland Publishing Company, Amsterdam, The Netherlands, 2014.

[12] K.A. Gschneidner, V.K. Pecharsky, Thirty years of near room temperature magnetic cooling: where we are today and future prospects, Int. J. Refrig. 31 (2008) 945–961, https://doi.org/10.1016/j.ijrefrig.2008.01.004.

[13] E. Brück, Developments in magnetocaloric refrigeration, J. Phys. D Appl. Phys. 38 (2005) R381, https://doi.org/10.1088/0022-3727/38/23/R01.

[14] A.M. Tishin, Y.I. Spichkin, The Magnetocaloric Effect and its Applications, IOP Publishing, Bristol, 2003.

[15] A.M. Tishin, Y.I. Spichkin, Relationship of adiabatic, isothermal and field constant changes of a magnetic entropy, AIP Conf. Proc. 614 (2002) 27–34, https://doi.org/10.1063/1.1472522.

[16] A.M. Tishin, Y.I. Spichkin, V.I. Zverev, P.W. Egolf, A review and new perspectives for the magnetocaloric effect: new materials and local heating and cooling inside the human body, Int. J. Refrig. 68 (2016) 177–186, https://doi.org/10.1016/j.ijrefrig.2016.04.020.

[17] O. Gutfleisch, M.A. Willard, E. Brück, C.H. Chen, S.G. Sankar, J.P. Liu, Magnetic materials and devices for the 21st century: stronger, lighter, and more energy efficient, Adv. Mater.. 23, 821–842. doi:10.1002/adma.201002180.

[18] C. Zimm, A. Jastrab, A. Sternberg, V. Pecharsky, K.G. Jr, M. Osborne, I. Anderson, Description and performance of a near-room temperature magnetic refrigerator, in: P. Kittel (Ed.), Advances in Cryogenic Engineering, Springer US, 1998, pp. 1759–1766, , https://doi.org/10.1007/978-1-4757-9047-4_222.

[19] N.A. Zarkevich, D.D. Johnson, V.K. Pecharsky, High-throughput search for caloric materials: the CaloriCool approach, J. Phys. D Appl. Phys. 51 (2018) 024002, https://doi.org/10.1088/1361-6463/aa9bd0.

[20] J.B. Chaudron, C. Muller, M. Hittinger, et al., Performance Measurements on a Large-Scale Magnetocaloric Cooling Application at Room Temperature, (2018), https://doi.org/10.18462/iir.thermag.2018.0022.

[21] A. Rowe, Configuration and performance analysis of magnetic refrigerators, Int. J. Refrig. 34 (2011) 168–177, https://doi.org/10.1016/j.ijrefrig.2010.08.014.

[22] B. Yu, M. Liu, P.W. Egolf, A. Kitanovski, A review of magnetic refrigerator and heat pump prototypes built before the year 2010, Int. J. Refrig. 33 (2010) 1029–1060, https://doi.org/10.1016/j.ijrefrig.2010.04.002.

[23] P. Weiss, A. Piccard, Le phénomène magnétocalorique, J. Phys. Theor. Appl. 7 (1917) 103–109, https://doi.org/10.1051/jphystap:019170070010300.

[24] A. Smith, Who discovered the magnetocaloric effect? EPJ H 38 (2013) 507–517, https://doi.org/10.1140/epjh/e2013-40001-9.

[25] P. Debye, Einige bemerkungen zur magnetisierung bei tiefer temperatur, Ann. Phys.. 386 (n.d.) 1154–1160. doi:10.1002/andp.19263862517.

[26] W.F. Giauque, A thermodynamic treatment of certain magnetic effects. A proposed method of producing temperatures considerably below 1° absolute, J. Am. Chem. Soc. 49 (1927) 1864–1870, https://doi.org/10.1021/ja01407a003.

[27] W.F. Giauque, D.P. MacDougall, Attainment of temperatures below 1 absolute by demagnetization of Gd2(SO4)3*8H2O, Phys. Rev. 43 (1933), https://doi.org/10.1103/PhysRev.43.768 768–768.

[28] G.V. Brown, Magnetic heat pumping near room temperature, J. Appl. Phys. 47 (1976) 3673–3680, https://doi.org/10.1063/1.323176.

[29] S.A. Nikitin, G. Myalikgulyev, A.M. Tishin, M.P. Annaorazov, K.A. Asatryan, A.L. Tyurin, The magnetocaloric effect in Fe49Rh51 compound, Phys. Lett. 148 (1990) 363–366, https://doi.org/10.1016/0375-9601(90)90819-A.

[30] J. Liu, T. Gottschall, K.P. Skokov, J.D. Moore, O. Gutfleisch, Giant magnetocaloric effect driven by structural transitions, Nat. Mater. 11 (2012) 620–626, https://doi.org/10.1038/nmat3334.

[31] A. Chirkova, K.P. Skokov, L. Schultz, N.V. Baranov, O. Gutfleisch, T.G. Woodcock, Giant adiabatic temperature change in FeRh alloys evidenced by direct measurements under cyclic conditions, Acta Mater. 106 (2016) 15–21, https://doi.org/10.1016/j.actamat.2015.11.054.

[32] J.B. Staunton, R. Banerjee, M. dos, S. Dias, A. Deak, L. Szunyogh, Fluctuating local moments, itinerant electrons, and the magnetocaloric effect: compositional hypersensitivity of FeRh, Phys. Rev. B 89 (2014) 054427, https://doi.org/10.1103/PhysRevB.89.054427.

[33] M. Takahashi, R. Oshima, Annealing effect on phase transition of equiatomic FeRh alloy, Mater. Trans., JIM 36 (1995) 735–742, https://doi.org/10.2320/matertrans1989.36.735.

[34] M.P. Annaorazov, K.A. Asatryan, G. Myalikgulyev, S.A. Nikitin, A.M. Tishin, A.L. Tyurin, Alloys of the Fe-Rh system as a new class of working material for magnetic refrigerators, Cryogenics 32 (1992) 867–872, https://doi.org/10.1016/0011-2275(92)90352-B.

[35] V.I. Zverev, A.M. Saletsky, R.R. Gimaev, A.M. Tishin, T. Miyanaga, J.B. Staunton, Influence of structural defects on the magnetocaloric effect in the vicinity of the first order magnetic transition in Fe50.4Rh49.6, Appl. Phys. Lett. 108 (2016) 192405, https://doi.org/10.1063/1.4949355.

[36] V.K. Pecharsky, K.A. Gschneidner Jr., Giant magnetocaloric effect in Gd5Si2Ge2, Phys. Rev. Lett. 78 (1997) 4494–4497, https://doi.org/10.1103/PhysRevLett.78.4494.

[37] V.K. Pecharsky, K.A. Gschneidner, Tunable magnetic regenerator alloys with a giant magnetocaloric effect for magnetic refrigeration from ~20 to ~290 K, Appl. Phys. Lett. 70 (1997) 3299–3301, https://doi.org/10.1063/1.119206.

[38] X.X. Zhang, J. Tejada, Y. Xin, G.F. Sun, K.W. Wong, X. Bohigas, Magnetocaloric effect in La0.67Ca0.33MnOδ and La0.60Y0.07Ca0.33MnOδ bulk materials, Appl. Phys. Lett. 69 (1996) 3596–3598, https://doi.org/10.1063/1.117218.

[39] Z.B. Guo, Y.W. Du, J.S. Zhu, H. Huang, W.P. Ding, D. Feng, Large magnetic entropy change in perovskite-type manganese oxides, Phys. Rev. Lett. 78 (1997) 1142–1145, https://doi.org/10.1103/PhysRevLett.78.1142.

[40] H. Feng-xia, S. Bao-gen, S. Ji-rong, Z. Xi-xiang, Great magnetic entropy change in La(Fe, M) 13 (M =Si, Al) with Co doping, Chin. Phys. 9 (2000) 550, https://doi.org/10.1088/1009-1963/9/7/016.

[41] A. Fujita, S. Fujieda, Y. Hasegawa, K. Fukamichi, Itinerant-electron metamagnetic transition and large magnetocaloric effects in La(FexSi1-x)13 compounds and their hydrides, Phys. Rev. B 67 (2003) 104416, https://doi.org/10.1103/PhysRevB.67.104416.

[42] H. Wada, Y. Tanabe, Giant magnetocaloric effect of MnAs1−xSbx, Appl. Phys. Lett. 79 (2001) 3302–3304, https://doi.org/10.1063/1.1419048.

[43] O. Tegus, E. Brück, K.H.J. Buschow, F.R. de Boer, Transition-metal-based magnetic refrigerants for room-temperature applications, Nature 415 (2002) 150–152, https://doi.org/10.1038/415150a.

[44] F. Hu, B. Shen, J. Sun, Magnetic entropy change in Ni51.5Mn22.7Ga25.8 alloy, Appl. Phys. Lett. 76 (2000) 3460–3462, https://doi.org/10.1063/1.126677.

[45] T. Krenke, E. Duman, M. Acet, E.F. Wassermann, X. Moya, L. Mañosa, A. Planes, Inverse magnetocaloric effect in ferromagnetic Ni–Mn–Sn alloys, Nat. Mater. 4 (2005) 450–454, https://doi.org/10.1038/nmat1395.

[46] E. Liu, W. Wang, L. Feng, W. Zhu, G. Li, J. Chen, H. Zhang, G. Wu, C. Jiang, H. Xu, F. de Boer, Stable magnetostructural coupling with tunable magnetoresponsive effects in hexagonal ferromagnets, Nat. Commun. 3 (2012) 873, https://doi.org/10.1038/ncomms1868.

[47] Y. Li, H. Zhang, K. Tao, Y. Wang, M. Wu, Y. Long, Giant magnetocaloric effect induced by reemergence of magnetostructural coupling in Si-doped Mn0.95CoGe compounds, Mater. Des. 114 (2017) 410–415, https://doi.org/10.1016/j.matdes.2016.11.002.

[48] V. Provenzano, A.J. Shapiro, R.D. Shull, Reduction of hysteresis losses in the magnetic refrigerant Gd5Ge2Si2 by the addition of iron, Nature 429 (2004) 853–857, https://doi.org/10.1038/nature02657.

[49] J. Lyubina, R. Schäfer, N. Martin, L. Schultz, O. Gutfleisch, Novel design of La(Fe,Si)13 alloys towards high magnetic refrigeration performance, Adv. Mater. 22 (2010) 3735–3739, https://doi.org/10.1002/adma.201000177 Weinheim.

[50] F. Guillou, G. Porcari, H. Yibole, N. van Dijk, E. Brück, Taming the first-order transition in giant magnetocaloric materials, Adv. Mater.. 26, 2671–2675. doi:10.1002/adma.201304788.

[51] V.I. Zverev, R.R. Gimaev, A.M. Tishin, Y. Mudryk, K.A. Gschneidner, V.K. Pecharsky, The role of demagnetization factor in determining the 'true' value of the Curie temperature, J. Magn. Magn Mater. 323 (2011) 2453–2457, https://doi.org/10.1016/j.jmmm.2011.05.012.

[52] H. Zhang, F. Hu, J. Sun, B. Shen, Effects of interstitial H and/or C atoms on the magnetic and magnetocaloric properties of La(Fe, Si)13-based compounds, Sci. China Phys. Mech. Astron. 56 (2013) 2302–2311, https://doi.org/10.1007/s11433-013-5357-1.

[53] W.F. Giauque, D.P. MacDougall, The production of temperatures below one degree absolute by adiabatic demagnetization of gadolinium sulfate, J. Am. Chem. Soc. 57 (1935) 1175–1185, https://doi.org/10.1021/ja01310a007.

[54] V.K. Pecharsky, K.A. Gschneidner, S.Y. Dan'kov, A.M. Tishin, Magnetocaloric properties of Gd3Al2, Cryocoolers 10, Springer, Boston, MA, 2002, pp. 639–645, , https://doi.org/10.1007/0-306-47090-X_76.

[55] M.D. Kuz'min, A.M. Tishin, Magnetic refrigerants for the 4.2-20 K region: garnets or perovskites? J. Phys. D Appl. Phys. 24 (1991) 2039, https://doi.org/10.1088/0022-3727/24/11/020.

[56] M.D. Kuz'min, A.M. Tishin, DyAlO3: a more promising refrigerant than Dy3Al5O12? J. Appl. Phys. 73 (1993) 4083–4085, https://doi.org/10.1063/1.352835.

[57] A.M. Tishin, L.P. Bozkova, New magnetic refrigerants for low temperature region, J. Appl. Phys. 81 (1997) 1000–1001, https://doi.org/10.1063/1.364191.

[58] S.Y. Dan'kov, V.V. Ivtchenko, A.M. Tishin, K.A. Gschneidner, V.K. Pecharsky, Magnetocaloric effect in GdAl2 and Nd2Fe17, Advances in Cryogenic Engineering Materials, Springer, Boston, MA, 2000, pp. 397–404, , https://doi.org/10.1007/978-1-4615-4293-3_51.

[59] K.A. GschneidnerJr, V.K. Pecharsky, A.O. Tsokol, Recent developments in magnetocaloric materials, Rep. Prog. Phys. 68 (2005) 1479, https://doi.org/10.1088/0034-4885/68/6/R04.

[60] D. Bloch, F. Chaissé, F. Givord, J. Voiron, E. Burzo, Étude des composés, type phase de laves, entre le cobalt et les terres rares paramagnétisme et effets de la pression, J. Phys. Colloq. 32 (1971), https://doi.org/10.1051/jphyscol:19711228 C1-659-C1-660.

[61] J. Voiron, D. Bloch, J. Phys. 32 (1971) 949 Paris.

[62] J. Herrero-Albillos, F. Bartolomé, L.M. García, F. Casanova, A. Labarta, X. Batlle, Entropy change at the magnetostructural transition in RCo2(R=Dy,Ho,Er), J. Magn. Magn Mater. 301 (2006) 378–382, https://doi.org/10.1016/j.jmmm.2005.07.032.

[63] S.A. Nikitin, A.M. Tishin, Magnetocaloric effect in HoCo2 compound, Cryogenics 31 (1991) 166–167, https://doi.org/10.1016/0011-2275(91)90171-R.

[64] N.H. Duc, T. Goto, Chapter 171 Itinerant electron metamagnetism of co sublattice in the lanthanide-cobalt intermetallics, Handbook on the Physics and Chemistry of Rare Earths, Elsevier, 1999, pp. 177–264, , https://doi.org/10.1016/S0168-1273(99)26006-0.

[65] S. Khmelevskyi, P. Mohn, The order of the magnetic phase transitions in RCo 2 (R = rare earth) intermetallic compounds, J. Phys. Condens. Matter 12 (2000) 9453, https://doi.org/10.1088/0953-8984/12/45/308.

[66] C. Kittel, Model of exchange-inversion magnetization, Phys. Rev. 120 (1960) 335–342, https://doi.org/10.1103/PhysRev.120.335.

[67] V.I. Zverev, A.M. Tishin, Z. Min, Y. Mudryk, K.A. Gschneidner, V.K. Pecharsky, Magnetic and magnetothermal properties, and the magnetic phase diagram of single-crystal holmium along the easy magnetization direction, J. Phys. Condens. Matter 27 (2015) 146002, https://doi.org/10.1088/0953-8984/27/14/146002.

[68] H. Zhang, B.G. Shen, Z.Y. Xu, J. Shen, F.X. Hu, J.R. Sun, Y. Long, Large reversible magnetocaloric effects in ErFeSi compound under low magnetic field change around liquid hydrogen temperature, Appl. Phys. Lett. 102 (2013) 092401, https://doi.org/10.1063/1.4794415.

[69] H. Zhang, Y.J. Sun, E. Niu, L.H. Yang, J. Shen, F.X. Hu, J.R. Sun, B.G. Shen, Large magnetocaloric effects of RFeSi (R = Tb and Dy) compounds for magnetic refrigeration in nitrogen and natural gas liquefaction, Appl. Phys. Lett. 103 (2013) 202412, https://doi.org/10.1063/1.4832218.

[70] Z. Hu, S. Bao-Gen, Magnetocaloric effects in RTX intermetallic compounds (R = Gd–Tm, T = Fe–Cu and Pd, X = Al and Si), Chin. Phys. B 24 (2015) 127504, https://doi.org/10.1088/1674-1056/24/12/127504.

[71] S. Gupta, K.G. Suresh, Review on magnetic and related properties of RTX compounds, J. Alloy. Comp. 618 (2015) 562–606, https://doi.org/10.1016/j.jallcom.2014.08.079.

[72] R. Welter, G. Venturini, B. Malaman, Magnetic properties of RFeSi (RLa-Sm, Gd-Dy) from susceptibility measurements and neutron diffraction studies, J. Alloy. Comp. 189 (1992) 49–58, https://doi.org/10.1016/0925-8388(92)90045-B.

[73] V.K. Pecharsky, K.A. Gschneidner, Magnetocaloric effect from indirect measurements: magnetization and heat capacity, J. Appl. Phys. 86 (1999) 565–575, https://doi.org/10.1063/1.370767.

[74] K.A. Gschneidner Jr., V.K. Pecharsky, A.O. Pecharsky, C.B. Zimm, Recent developments in magnetic refrigeration, Rare Earths '98, Trans Tech Publications, 1999, pp. 69–76, , https://doi.org/10.4028/www.scientific.net/MSF.315-317.69.

[75] A. Giguère, M. Foldeaki, B. Ravi Gopal, R. Chahine, T.K. Bose, A. Frydman, J.A. Barclay, Direct measurement of the "Giant" adiabatic temperature change in Gd5Si2Ge2, Phys. Rev. Lett. 83 (1999) 2262–2265, https://doi.org/10.1103/PhysRevLett.83.2262.

[76] K.A. Gschneidner, V.K. Pecharsky, E. Brück, H.G.M. Duijn, E.M. Levin, Direct measurement of the 'Giant' adiabatic temperature change in Gd5Si2Ge2, Phys. Rev. Lett. 85 (2000), https://doi.org/10.1103/PhysRevLett.85.4190 4190–4190.

[77] J.-D. Zou, B.-G. Shen, B. Gao, J. Shen, J.-R. Sun, The magnetocaloric effect of LaFe11.6Si1.4, La0.8Nd0.2Fe11.5Si1.5, and Ni43Mn46Sn11 compounds in the vicinity of the first-order phase transition, Adv. Mater.. 21, 693–696. doi:10.1002/adma.200800955.

[78] L. Mañosa, A. Planes, X. Moya, Comment on "the magnetocaloric effect of LaFe11.6Si1.4, La0.8Nd0.2Fe11.5Si1.5, and Ni43Mn46Sn11 compounds in the vicinity of the first-order phase transition," Adv. Mater.. 21 (n.d.) 3725–3726. doi:10.1002/adma.200900688.

[79] L. Caron, Z.Q. Ou, T.T. Nguyen, D.T. Cam Thanh, O. Tegus, E. Brück, On the determination of the magnetic entropy change in materials with first-order transitions, J. Magn. Magn Mater. 321 (2009) 3559–3566, https://doi.org/10.1016/j.jmmm.2009.06.086.

[80] J.S. Amaral, V.S. Amaral, On estimating the magnetocaloric effect from magnetization measurements, J. Magn. Magn Mater. 322 (2010) 1552–1557, https://doi.org/10.1016/j.jmmm.2009.06.013.

[81] V.I. Zverev, A.M. Tishin, M.D. Kuz'min, The maximum possible magnetocaloric ΔT effect, J. Appl. Phys. 107 (2010) 043907, https://doi.org/10.1063/1.3309769.

[82] X.X. Zhang, F.W. Wang, G.H. Wen, Magnetic entropy change in RCoAl (R = Gd, Tb, Dy, and Ho) compounds: candidate materials for providing magnetic refrigeration in the temperature range 10 K to 100 K, J. Phys. Condens. Matter 13 (2001) L747, https://doi.org/10.1088/0953-8984/13/31/102.

[83] N.K. Singh, D. Paudyal, V.K. Pecharsky, K.A. Gschneidner, Magnetic and magnetothermodynamic properties of Ho5Si4, J. Appl. Phys. 107 (2010), https://doi.org/10.1063/1.3365515 09A921.

[84] K. Ahn, A.O. Pecharsky, K.A. Gschneidner, V.K. Pecharsky, Preparation, heat capacity, magnetic properties, and the magnetocaloric effect of EuO, J. Appl. Phys. 97 (2005) 063901, https://doi.org/10.1063/1.1841463.

[85] H. Zhang, Y.J. Sun, L.H. Yang, E. Niu, H.S. Wang, F.X. Hu, J.R. Sun, B.G. Shen, Successive inverse and normal magnetocaloric effects in HoFeSi compound, J. Appl. Phys. 115 (2014) 063901, https://doi.org/10.1063/1.4865297.

[86] A. Smith, C.R.H. Bahl, R. Bjørk, K. Engelbrecht, K.K. Nielsen, N. Pryds, Materials challenges for high performance magnetocaloric refrigeration devices, Adv. Energy Mater. 2 (2012) 1288–1318, https://doi.org/10.1002/aenm.201200167.

[87] L.D. Griffith, Y. Mudryk, J. Slaughter, V.K. Pecharsky, Material-based figure of merit for caloric materials, J. Appl. Phys. 123 (2018) 034902, https://doi.org/10.1063/1.5004173.

[88] A.M. Tishin, Magnetic refrigeration in the low-temperature range, J. Appl. Phys. 68 (1990) 6480–6484, https://doi.org/10.1063/1.347186.

[89] A. Smaïli, R. Chahine, Composite materials for Ericsson-like magnetic refrigeration cycle, J. Appl. Phys. 81 (1997) 824–829, https://doi.org/10.1063/1.364166.

[90] B.J. Korte, V.K. Pecharsky, K.A. Gschneidner, The correlation of the magnetic properties and the magnetocaloric effect in (Gd1 − xErx)NiAl alloys, J. Appl. Phys. 84 (1998) 5677–5685, https://doi.org/10.1063/1.368830.

[91] H. Zhang, Z.Y. Xu, X.Q. Zheng, J. Shen, F.X. Hu, J.R. Sun, B.G. Shen, Magnetic properties and magnetocaloric effects in Gd1 − xHoxNiIn intermetallic compounds, Solid State Commun. 152 (2012) 1734–1738, https://doi.org/10.1016/j.ssc.2012.06.029.

[92] T. Hashimoto, T. Kuzuhara, M. Sahashi, K. Inomata, A. Tomokiyo, H. Yayama, New application of complex magnetic materials to the magnetic refrigerant in an Ericsson magnetic refrigerator, J. Appl. Phys. 62 (1987) 3873–3878, https://doi.org/10.1063/1.339232.

[93] S. Jeong, AMR (Active Magnetic Regenerative) refrigeration for low temperature, Cryogenics 62 (2014) 193–201, https://doi.org/10.1016/j.cryogenics.2014.03.015.

[94] G. Lorusso, J.W. Sharples, E. Palacios, O. Roubeau, E.K. Brechin, R. Sessoli, A. Rossin, F. Tuna, E.J.L. McInnes, D. Collison, M. Evangelisti, A dense metal–organic framework for enhanced magnetic refrigeration, Adv. Mater. 25 (2013) 4653–4656, https://doi.org/10.1002/adma.201301997.

[95] G. Lorusso, M.A. Palacios, G.S. Nichol, E.K. Brechin, O. Roubeau, M. Evangelisti, Increasing the dimensionality of cryogenic molecular coolers: Gd-based polymers and metal–organic frameworks, Chem. Commun. 48 (2012) 7592–7594, https://doi.org/10.1039/C2CC33485B.

[96] N.K. Singh, S. Gupta, V.K. Pecharsky, V.P. Balema, Solvent-free mechanochemical synthesis and magnetic properties of rare-earth based metal-organic frameworks, J. Alloy. Comp. 696 (2017) 118–122, https://doi.org/10.1016/j.jallcom.2016.11.220.

[97] Y.I. Spichkin, A.K. Zvezdin, S.P. Gubin, A.S. Mischenko, A.M. Tishin, Magnetic molecular clusters as promising materials for refrigeration in low-temperature regions, J. Phys. D Appl. Phys. 34 (2001) 1162, https://doi.org/10.1088/0022-3727/34/8/306.

[98] P.E. Blumenfeld, F.C. Prenger, A. Sternberg, C. Zimm, High temperature superconducting magnetic refrigeration, AIP Conf. Proc. 613 (2002) 1019–1026, https://doi.org/10.1063/1.1472124.

[99] A. Tura, A. Rowe, Permanent magnet magnetic refrigerator design and experimental characterization, Int. J. Refrig. 34 (2011) 628–639, https://doi.org/10.1016/j.ijrefrig.2010.12.009.

[100] V. Franco, J.S. Blázquez, J.J. Ipus, J.Y. Law, L.M. Moreno-Ramírez, A. Conde, Magnetocaloric effect: from materials research to refrigeration devices, Prog. Mater. Sci. 93 (2018) 112–232, https://doi.org/10.1016/j.pmatsci.2017.10.005.

[101] Y. Hakuraku, H. Ogata, A static magnetic refrigerator for superfluid helium with new heat switches and a superconducting pulse coil, Jpn. J. Appl. Phys. 24 (1985) 1538, https://doi.org/10.1143/JJAP.24.1538.

[102] A. Bézaguet, J. Casas-Cubillos, P. Lebrun, R. Losserand-Madoux, M. Marquet, M. Schmidt-Ricker, P. Seyfert, Design and construction of a static magnetic refrigerator operating between 1.8 K and 4.5 K, Cryogenics 34 (1994) 227–230, https://doi.org/10.1016/S0011-2275(05)80049-9.

[103] A. Kashani, B.P.M. Helvensteijn, F.J. McCormack, A.L. Spivak, Performance of a magnetic refrigerator operating between 2 K and 10 K, Advances in Cryogenic Engineering, Springer, Boston, MA, 1996, pp. 1313–1320, , https://doi.org/10.1007/978-1-4613-0373-2_165.

[104] J. Bartlett, G. Hardy, I.D. Hepburn, Performance of a fast response miniature Adiabatic Demagnetisation Refrigerator using a single crystal tungsten magnetoresistive heat switch, Cryogenics 72 (2015) 111–121, https://doi.org/10.1016/j.cryogenics.2015.10.004.

[105] L. Zhang, S.A. Sherif, A.J. DeGregoria, C.B. Zimm, T.N. Veziroglu, Design optimization of a 0.1-ton/day active magnetic regenerative hydrogen liquefier, Cryogenics 40 (2000) 269–278, https://doi.org/10.1016/S0011-2275(00)00039-4.

[106] Y. Kim, I. Park, S. Jeong, Experimental investigation of two-stage active magnetic regenerative refrigerator operating between 77K and 20K, Cryogenics 57 (2013)

113–121, https://doi.org/10.1016/j.cryogenics.2013.06.002.
[107] I. Park, S. Jeong, Experimental investigation of 20 K two-stage layered active magnetic regenerative refrigerator, IOP Conf. Ser. Mater. Sci. Eng. 101 (2015) 012106, https://doi.org/10.1088/1757-899X/101/1/012106.
[108] K. Matsumoto, T. Kondo, M. Ikeda, T. Numazawa, Numerical analysis of active magnetic regenerators for hydrogen magnetic refrigeration between 20 and 77K, Cryogenics 51 (2011) 353–357, https://doi.org/10.1016/j.cryogenics.2010.06.003.
[109] T. Numazawa, K. Kamiya, S. Yoshioka, H. Nakagome, K. Matsumoto, Development of a magnetic refirgerator for hydrogen liquefaction, AIP Conf. Proc. 985 (2008) 1183–1189, https://doi.org/10.1063/1.2908470.
[110] J. Park, S. Jeong, I. Park, Development and parametric study of the convection-type stationary adiabatic demagnetization refrigerator (ADR) for hydrogen re-condensation, Cryogenics 71 (2015) 82–89, https://doi.org/10.1016/j.cryogenics.2015.06.006.